

Low energy structures in nuclear reactions with 4n in the final state

¹Rimantas Lazauskas

¹ *Université de Strasbourg, CNRS, IPHC UMR 7178, F-67000 Strasbourg, France*

^{2,3}Emiko Hiyama

²*Department of Physics, Kyushu University, Fukuoka, 819-0395, Japan and*

³*RIKEN Nishina Center, Wako 351-0198 Japan*

⁴Jaume Carbonell

⁴ *Université Paris-Saclay, CNRS/IN2P3, IJCLab, 91405 Orsay, France*

(Dated: July 18, 2022)

We present a reaction model to describe the fast removal of the α -particle core in ${}^8\text{He}$ nucleus with eventual emission of four neutrons. The obtained four neutron energy distributions allows to explain the sharp low energy peak observed by studying the missing mass spectra of four neutrons in [Nature Vol. 606, p. 678], as a consequence of dineutron-dineutron correlations.

The possible existence of 3n and 4n bound and/or resonant states has been considered in the nuclear physics community since the 60's. The interest in this topic was however boosted at the beginning of this century by the experimental findings at GANIL [1] and at RIKEN [2] claiming a positive signal of a bound [1] or a nearthreshold resonant [2] tetraneutron, though compatible with each other within the error bars.

If the existence of bound three- or four-neutron states are totally excluded from the theoretical point of view [11–13], and seems also be the case by most of the experimental studies [36], during the past twenty years there has been a long debate about the possibility of observable multineutron resonances. An attempt to reviewing this activity, both from the theoretical and experimental points of view, can be found in [5].

For the authors of the present article, the possibility of observing a 3n and 4n resonances, a fortiori bound states, are also totally excluded [6–10, 35]. Our first two works [6, 7] were motivated by the surprising and somehow contradictory results of Ref. [13] in which the author excluded – by far – any 4n bound state but suggested the possibility of a 4n nearthreshold resonance. The relevant question to us was not to discuss whether or not 3n and 4n resonances – considered as S-matrix poles in the complex energy manifold – existed [37], but to determine as precisely as possible their position, mainly their proximity to the physical region. To this aim we developed in collaboration with our RIKEN colleagues, independent rigorous *ab-initio* methods to solve the 3 and 4 body problems in the continuum. Thus, the positions of the lowest 3n and 4n resonances were effectively computed by using several realistic nn potentials and found to be in all cases very far from the real axis with no possibility of manifesting in any scattering observable.

This was also the conclusion of a long series of theoretical works, considering properly asymptotic behavior of unbound systems [15–22]. As well it is a direct, and model independent, consequence of EFT in the unitary limit [23–25] predicting strong repulsion between

two identical difermions in the total angular momentum $J = 0^+$ state, which represents by far the most favorable configuration to form four fermion states. It is worth noticing however that other theoretical works [26–28] persisted in the line of [13] and claimed 4n resonant states with parameters $E_R \sim \Gamma \sim 1\text{--}2$ MeV. To our humble opinion this discrepancy might be result of disregarding long range dineutron correlations in the last set of papers, crucial component in describing multineutron dynamics [18].

A very recent publication [3], involving several experimental groups, reports evidence of a low energy structure in the quasi-elastic reaction ${}^8\text{He}(p, p^4\text{He})4n$ performed at RIKEN. This remarkable study indeed provides the first convincing signal on a nearthreshold structure in a nuclear reaction with 4n neutron in the final state. The signal, composed of two well-separated peaks at $E \approx 2$ MeV and at $E \approx 30$ MeV respectively, is observed in the missing mass spectrum of the four-neutron system. Assuming a Breit-Wigner form, it is suggested that the first peak could provide a direct indication of a 4n resonance with parameters $E_R=2.37\pm 0.38\pm 0.44$ MeV and $\Gamma=1.75\pm 0.22\pm 0.30$ MeV. Their analysis, based on the COSMA model [14] which assumes a sudden removal of the alpha-particle core from ${}^8\text{He}$ and a flat (democratic) distribution of the four neutron final state, provided an almost perfect description of the broad structure, but found no explanation for the sharp low energy peak. One should notice, however, that the authors of Ref. [29], employing the same model, observed a strong dependence of the multineutron response on their initial distribution as well as on the final state interactions in shifting the peak to lower energies. This last study was however unable to describe four neutrons emission in 2n+2n configurations.

Indeed, with the same strength that we have excluded any 3n and 4n resonance we [6–10], together with other authors [16, 19, 29], have insistently claimed that such a low energy structure could indeed manifest itself in low energy process as a consequence of neutron's final state and the reaction mechanism, without any link with an

underlying 4n resonant state. Maybe the most trivial illustrative example can be found in Figure 21 of Ref [5] where a similar structure is produced by a two-body repulsive well in P-wave.

The present letter aims to build a realistic dynamical model of the ${}^8\text{He}(p, p^4\text{He})4n$ reaction, explaining the low energy structure reported in [3], bridging the gap between the conflicting views in theory and experiment. We will show that the experimental results displayed in Fig. 3 of Ref. [3] find a natural explanation in terms of the dineutron correlations in the final state, if four neutrons are weakly bound in an initial projectile and form broad wave function.

In this study, the ${}^8\text{He}$ target is considered as a ${}^4\text{He}+nnnn$ system, in such a way that the 4n preexists confined in the field of the remaining nucleons from the ${}^4\text{He}$ core, supposed to be fixed in the center of mass of the four valence neutrons.

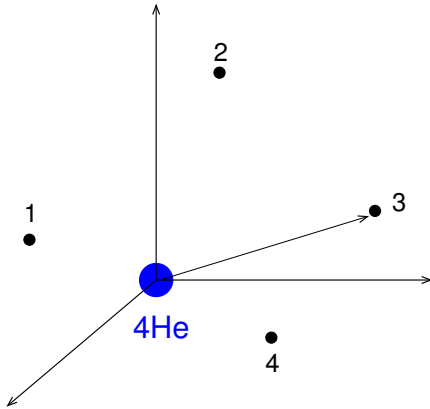


FIG. 1: ${}^8\text{He}$ described as a four neutron system orbiting around an infinitely heavy ${}^4\text{He}$ core.

The Hamiltonian of the initial state is given by

$$H_i = H_0 + \sum_{i<j=1}^4 V_{nn}(r_{ij}) + \sum_{i=1}^4 V_{iG}(r_i) + \sum_{i<j=1}^4 W_{ijG}, \quad (1)$$

where H_0 is the 4n kinetic energy, V_{nn} is the neutron-neutron interaction depending on the interparticle distance $r_{ij} = |\vec{r}_i - \vec{r}_j|$,

$$V_{nG}(\vec{r}_i) = V_0 e^{-[(\vec{r}_i - \vec{R}_G)/\rho_0]^2}, \quad (2)$$

is the mean-field centered on the center of mass of the ${}^8\text{He}$ (\vec{R}_G), that is on the ${}^4\text{He}$ core, acting on each neutron with position \vec{r}_i and

$$W_{ijG}(\rho) = r_{ijG} W_0 e^{-[\rho/\rho_0]^2}; \quad \rho^2 = [r_{ij}/4]^2 + r_{ijG}^2/2, \quad (3)$$

is a three-body force acting between two neutrons and the ${}^4\text{He}$ core, with $r_{ijG} = (\vec{r}_i + \vec{r}_j)/2 - \vec{R}_G$ denoting the

distance between center of mass of a neutron pair (ij) and the core. We will hereafter set $\vec{R}_G = 0$.

The strength of the interaction ($V_0(\rho_0)$) is adjusted to reproduce the binding energy of two valence neutrons in ${}^6\text{He}$ ($B_{{}^4\text{He}}^{2n} = B_{{}^6\text{He}} - B_{{}^4\text{He}} = 0.97$ MeV). Note that in our model for ${}^6\text{He}$, the distance $r_{ijG} = 0$ and W_{ijG} interaction does not contribute ($W_{ijG} \equiv 0$). The strength parameter (W_0) is then adjusted to reproduce the binding energy of valence neutrons in ${}^8\text{He}$ ($B_{{}^4\text{He}}^{4n} = B_{{}^8\text{He}} - B_{{}^4\text{He}} = 3.11$ MeV).

The initial state $|\Psi_i\rangle$, representing the ${}^8\text{He}$ nucleus, is provided by a solution of the Schrödinger equation

$$H_i |\Psi_i\rangle = E_i |\Psi_i\rangle. \quad (4)$$

In practice, it has been obtained by solving corresponding four-body Faddeev-Yakubovsky (FY) equations in configuration space as described in [30].

We will assume that the ${}^8\text{He}$ projectile is broken by a sudden removal of the ${}^4\text{He}$ -core, reflecting well the configuration of the experiment [3], realized with a 156 MeV per nucleon ${}^8\text{He}$ beam. Thus, at the moment of the core removal, the distribution of four neutrons coincides with that of the valence neutrons present in ${}^8\text{He}$. The wave function of these neutrons is driven by the four-body Hamiltonian:

$$H_f = H_0 + \sum_{i<j=1}^4 V_{nn}(r_{ij}). \quad (5)$$

The final state, $|\Phi_f\rangle$, corresponds to the 4n in the continuum with total energy E_{4n} , and is a solution of

$$H_f |\Phi_f\rangle = E_{4n} |\Phi_f\rangle. \quad (6)$$

Next step is to obtain the response (or strength) function $S(E)$ corresponding to the process

$$A \equiv \langle {}^4\text{He} \Phi_{4n}(E) | \hat{O} | {}^8\text{He} \rangle = \langle \Phi_f | \hat{O} | \Psi_i \rangle, \quad (7)$$

where \hat{O} is some transition operator representing effect of α -core removal on the initial configuration of the four valence neutrons. In the first approximation, one may assume that α -core is removed without affecting peripheral neutrons present in the halo and thus $\hat{O} = 1$.

The response function $S(E)$ is given by [10]

$$S_{4n}(E) = \sum_{\nu} \left| \langle \Psi_{\nu} | \hat{O} | \Psi_i \rangle \right|^2 \delta(E - E_{\nu}), \quad (8)$$

where Ψ_i denotes the ground state wave function of the ${}^8\text{He}$ nucleus, with ground-state energy E_i , and Ψ_{ν} represents the wave function of the 4n system in the continuum with an energy E_{ν} . Both wave functions are solutions of the corresponding four-nucleon Hamiltonians H_i, H_f . The energy is measured from some standard value, e.g. a particle-decay threshold energy.

The strength function (8) may be rewritten in terms of the forward propagator

$$\hat{G}^+(E) = \frac{1}{E - \hat{H} + i\epsilon}, \quad (9)$$

in the following form

$$S_{4n}(E) = -\frac{1}{\pi} \text{Im} \left\langle \Psi_i \left| \hat{O}^\dagger \hat{G}^+(E) \hat{O} \right| \Psi_i \right\rangle, \quad (10)$$

in which the summation over the final states is avoided.

The later expression can still be transformed into

$$S_{4n}(E) = -\frac{1}{\pi} \text{Im} \left\langle \Psi_i \left| \hat{O}^\dagger \left| \bar{\Phi}_f(E) \right. \right. \right\rangle. \quad (11)$$

that is, as a matrix element of the of the (conjugate) transition operator between the initial state Ψ_i and the the outgoing collision wave-function $\bar{\Phi}_f(E)$, defined as

$$\bar{\Phi}_f(E) = \hat{G}^+(E) \hat{O} \Psi_i. \quad (12)$$

Naturally, this wave function is a solution of the inhomogeneous equation

$$(E - \hat{H}_f + i\epsilon) \bar{\Phi}_f(E) = \hat{O} \Psi_i, \quad (13)$$

at a chosen energy E .

The right-hand side of the former equation is compact, damped by the bound-state Ψ_i wave function. The wave function $\bar{\Phi}_f$ asymptotically contains only outgoing waves. However, the asymptotic structure of this wave function is rather complicated, involving multidimensional four-neutron break-up amplitudes. Nevertheless the last inhomogeneous equation may be comfortably solved using the complex scaling techniques, as explained in [10, 34]. Notably, to perform the numerical calculations, we will apply the same techniques as described in detail in our former articles.

In complement with the phenomenologically n - ^4He interaction introduced in the previous sections, we have considered two different nn potentials: the realistic AV18 [31], providing the low energy parameters $a_{nn} = -18.8$ fm and $r_0 = 2.83$ fm and the CD version of MT13 S-wave interaction [32] giving $a_{nn} = -18.6$ fm and $r_0 = 2.93$ fm. As we pointed out in [6–10] none of the aforementioned Hamiltonians support a $4n$ nearthreshold resonant states that could generate a low energy peak. Furthermore, the purely S-wave MT13 model, providing a_{nn} values much larger than the range of nuclear interaction, fully complies with the Effective Field Theory predictions in the unitary limit [23–25], which indicates the absence of an attractive interaction between two resonant fermionic pairs.

Our first task was to determine the parameters that reproduce, within our model, the experimental neutron separation energies $B_{^4\text{He}}^{2n} = 0.97$ MeV and $B_{^4\text{He}}^{4n} = 3.11$ MeV. Their values, when the nn AV18 potential is used, are provided in Table I, together with the calculated rms point radii of the halo neutron in ^8He . We may estimate the rms radius of this halo neutron from the *ab-initio* calculation of ^8He ground state provided by the Green function Monte Carlo method of Ref. [33] with AV18/IL2 Hamiltonian, as

$$6 \langle r_{nn}^2 \rangle_{^8\text{He}} - 2 \langle r_{nn}^2 \rangle_\alpha \lesssim 4 \langle r_{nn}^2 \rangle < 6 \langle r_{nn}^2 \rangle_{^8\text{He}}. \quad (14)$$

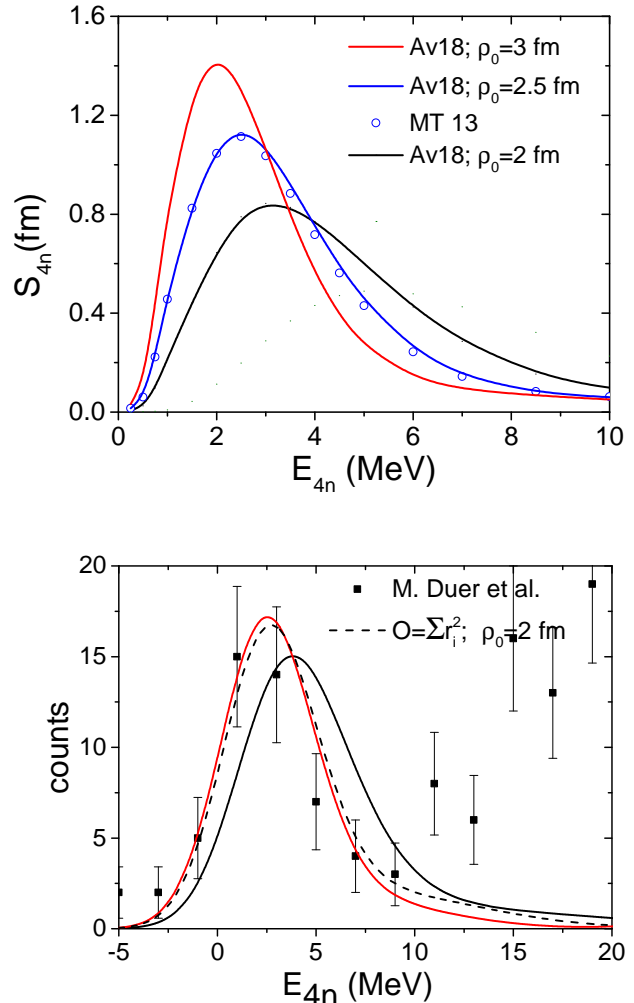


FIG. 2: The low energy response function of the $4n$ removed from ^8He is displayed as a function of its energy E_{4n} (upper panel). Different ranges of the n - ^4He interaction have been considered: $\rho_0=2$ fm (black), $\rho_0=2.5$ fm (blue) and $\rho_0=3$ fm (red), demonstrating the strong sensitivity of the response function to the neutrons initial distribution inside ^8He . The comparison between the MT 13 (blue points) and AV18 (solid blue line) models show the independence of the results with respect to the considered nn interaction. On the lower panel, we compare our prediction for neutron missing mass spectrum at low energy with the experimental results of ref.[3]. To this aim, the theoretical response functions have been broadened, taking into account the experimental energy resolution, and normalized to the number of observed counts below $E_{4n}=10$ MeV. Color coding is the same as in the upper panel figure.

The first inequality is obtained by supposing that ^4He -core remains unaffected by the presence of the halo neutrons in ^8He . In reality, however, the four valence neutrons slightly deform the ^4He core by attracting core-protons and compressing core-neutrons, which leads to the second inequality. Finally, one should ex-

pect $\langle r_{nn}^2 \rangle^{\frac{1}{2}} = 3.5\text{-}3.6$ fm.

The four neutron strength function (8) has been computed with these ingredients and is displayed in Figure 2 for three different parameterizations of the phenomenological interaction used to generate the initial distribution of the four neutrons, after the ${}^4\text{He}$ removal from ${}^8\text{He}$. One may see that, independently of the model parameters, one obtains a sharp neutron missing mass distribution peak at low energy. The centroid and width of this peak is strongly correlated with the rms radii of the neutron initial distribution, being pushed to lower energy if a more peripheral neutron distribution is generated in the initial state. This fact is in agreement with the observation made in [29]. However, our obtained distributions are much sharper and they are centered at considerably lower energies, indicating the importance of the $2n+2n$ decay channels, which were not taken into account in [29].

Furthermore, we found that our results are independent of the nn interaction model, as long as these models reproduce the same nn scattering length. This feature is demonstrated by comparing the solid blue curve, based on AV18 interaction, with the blue points, corresponding to the simplistic MT13 $4n$ Hamiltonian. Notably, the predictions of these two models differ by less than 2% at the peak of the distribution. This implies a negligible effect of nn interactions beyond S-wave, as expected from Effective field theory arguments.

Finally, in order to compare our results with a measurement of Ref. [3], we broadened our computed neutron strength distributions by the experimental resolution of 2 MeV and normalized their heights in order to be consistent with 54 events observed in the neutron missing-mass window $E_{4n} < 10$ MeV (see Fig 3 from [3]). Our results are shown in the lower panel of Fig 2. As one can see, we were able to obtain an excellent description of the low energy peak centered at around $E_{4n} \approx 2$ MeV. This is achieved with a Gaussian range parameter $\rho_0 = 3$ fm (solid red line). The black line corresponds to the smallest Gaussian range parameter $\rho_0 = 2$ fm, which describes the most compact four neutron distribution, just after the sudden removal of ${}^4\text{He}$ -core. This results into a more dilute four-neutron missing mass distribution than the observed experimentally.

One could argue that $\rho_0 = 2$ fm results are based on a more realistic neutron distribution in the initial state than $\rho_0 = 3$ fm, since the point rms radius is closer to the estimated one from the *ab-initio* calculation of Ref. [33]. A more detailed analysis of these neutron distributions reveals [38] that the interaction range ρ_0 mostly acts in separating $2n+2n$ clusters in the wave function of ${}^8\text{He}$. Our ${}^8\text{He}$ model is simplistic and does not take into account the Pauli principle between the ${}^4\text{He}$ -core and the four valence neutrons, which should naturally enhance the $2n+2n$ cluster separation. Moreover, one may expect that the full reaction mechanism enhance, on average, the contribution of the peripheral neutrons to the low energy part of the response function. Actually, the neutrons residing close to the core are more energetic and

correlate stronger with the core. They may gain some momenta with the core removal, propelling their contribution in to the high energy peak of the missing mass spectra. To mimic this effect, we have inserted in eq. (7) a transition operator of the form $\hat{O} = \sum_i r_i^2$. Such an operator is expected at second order approximation in the sudden core-removal for a $J^\pi = 0^+$ four neutron final state. As revealed by the black dashed line, corresponding to a Gaussian range parameter $r_0 = 2$ fm, the four neutron response approaches the experimental signal and turns to be very similar to the one obtained with $r_0 = 3$ fm and $\hat{O} = 1$.

In order to demonstrate the impact of the dineutron-dineutron correlations on the four neutron missing mass distribution, we have readjusted the MT 13 potential to generate different nn scattering length values : $a_{nn} = -40$ fm, $a_{nn} = -8$ fm and $a_{nn} = -2$ fm. This was achieved by scaling the originally used MT13 potential by a factor $\gamma = 1.05172$, $\gamma = 1.654$ and $\gamma = 0.5685$ respectively. We have also refit the phenomenological α -neutron interactions for $\rho_0=2.5$ fm, as previously, by adjusting the strength parameters V_0 and W_0 in order to reproduce the proper binding energies of ${}^6\text{He}$ and ${}^8\text{He}$. While by reducing the nn interactions, the strength calculated rms radii of valence neutrons slightly increase, this does not help to displace the neutron energy distributions to lower energies. On the contrary, the neutron energy distributions indicate strong inverse correlation with the size of the nn scattering length. As the nn interaction approaches the unitary limit ($a_{nn} = \pm\infty$), the neutron energy distribution becomes more and more pronounced. On the other hand, if the nn scattering length becomes non-resonant (i.e. $a_{nn} = -2$ fm) the strength function flattens, while its centroid is pushed to the 5 MeV region. Decreasing the a_{nn} from -18.6 fm to -8 fm displaces the $4n$ strength function peak by more than 0.5 MeV. This strong dependence of the four neutron missing mass distribution on the nn scattering length could be employed to determine the a_{nn} from the experimental data of the ${}^8\text{He}(p, p^4\text{He})4n$ reaction, if at some point the experiment energy resolution is improved. In order to constrain the theoretical results, a more accurate ${}^8\text{He}$ wave function, if possible from eight-body *ab-initio* calculations, might be used to determine the neutron distributions just after ${}^4\text{He}$ -core removal.

In summary, the recent experiment performed in RIKEN [3] found a remarkably sharp low energy structure in the missing mass distribution of four neutrons emitted in the quasi-elastic reaction knock-out ${}^8\text{He}(p, p^4\text{He})4n$. The authors of this experiment have not found an explanation for this phenomenon, though managing to describe successfully $4n$ distribution at higher energies as well as the presence of a low energy signal in a similar decay of ${}^6\text{He}$. As a possible explanation, the existence of a low-energy four-neutron resonant state has been suggested, thus challenging the theoretical understanding of the four-neutron system.

ρ_0 (fm)	V_0 (MeV)	W_0 (MeV fm $^{-1}$)	$\langle r_{nn}^2 \rangle^{\frac{1}{2}}$ (fm)
2.0	-2.4038	-0.3345	4.12
2.5	-1.9055	-0.2005	4.77
3.0	-1.6113	-0.1351	5.39
[33]			3.5-3.6

TABLE I: Strength parameters of the phenomenological α -core neutron interactions (described in section ??) as a function of interaction range ρ_0 , adjusted to reproduce binding of neutron halos in ${}^6\text{He}$ and ${}^8\text{He}$ nuclei. In the last column calculated halo neutron radii in ${}^8\text{He}$ are presented and compared with an estimation from *ab-initio* calculation of ref. [33] using expression of eq. (14).

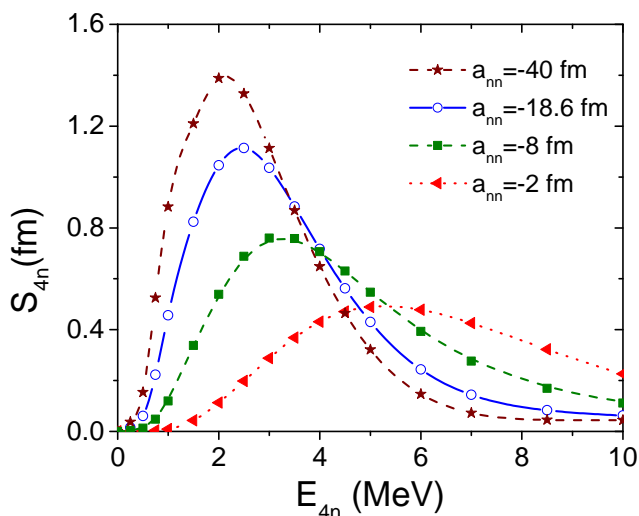


FIG. 3: Four neutrons response functions at low energy calculated for nn interaction in 1S_0 wave adjusted to reproduce scattering lengths of different size.

Motivated by these astonishing experimental results, we have constructed a realistic reaction model to describe the sudden α -particle removal from ${}^8\text{He}$. The model is based on a transition between the ${}^4\text{He}+4n$ initial state and the four interacting neutrons in the final one. A rigorous calculation allows us to determine the energy distributions of the four remaining neutrons in the final

state, which is found in close agreement with the experimental data. We have found, in this way, a natural explanation for the low energy structure observed in [3], which appears to be a consequence of the final state interaction among the $4n$ and the α -important presence of pre-existing four neutrons in the periphery of ${}^8\text{He}$ nucleus projectile.

Finally, a strong correlation is observed between the neutron missing mass spectrum in the ${}^8\text{He}(p, p^4\text{He})4n$ reaction and the value a_{nn} of the nn scattering length. If the energy resolution in such experiments could be improved, one may use the collected data to further constrain the not so well known a_{nn} value.

Acknowledgments. This research, started during the program Living Near Unitarity at the Kavli Institute for Theoretical Physics (KITP), University of Santa Barbara (California) is supported in part by the National Science Foundation under Grant No. NSF PHY-1748958. We thank the organizers and the staff members of this Institute for their invitation and financial support. We have benefited by french IN2P3 for a theory project "Neutron-rich light unstable nuclei" and by the Japanese Grant-in-Aid for Scientific Research on Innovative Areas (No.18H05407). We also profited from enriching discussions during ECT* NPES 2022 workshop in Trento, thanking ECT* for a partial support RL and EH stay. We were granted access to the HPC resources of TGCC/IDRIS under the allocation A0110506006 made by GENCI (Grand Equipement National de Calcul Intensif).

[1] F.M. Marqués et al., Phys. Rev. C **65**, 044006 (2002).
[2] K. Kisamori et al., Phys. Rev. Lett. **116**, 052501 (2016).
[3] M. Duer et al., Nature Vol 606, June 2022, page 678
[4] Th. Faestermann et al, Phys. Lett. B 824 (2022) 136799
[5] F. M. Marqués, J. Carbonell, Eur. Phys. J. A (2021) 57:105
[6] R. Lazauskas and J. Carbonell, Phys. Rev. C **71**, 044004 (2005).
[7] R. Lazauskas and J. Carbonell, Phys. Rev. C **72**, 034003

(2005).
[8] E. Hiyama et al, Phys. Rev. C **93**, 044004 (2016).
[9] J. Carbonell et al, Few-Body Syst. **58**, 67 (2017).
[10] R. Lazauskas et al, Prog. Theor. Exp. Phys. **2017**, 073D03 (2017).
[11] S.A. Sofianos, S.A. Rakityansky, and G.P. Vermaak, J. Phys. G **23** (1997) 1619
[12] N.K. Timofeyuk, J.Phys. G **29** (2003) L9
[13] S.C. Pieper, Phys. Rev. Lett. **90**, 252501 (2003).

- [14] M.V. Zhukov, A.A. Korshennikov, M.H. Smedberg, Phys. Rev. C 50, R1 (1994).
- [15] A. Deltuva, Phys. Rev. C **97**, 034001 (2018).
- [16] A. Deltuva, Phys. Lett. B **782**, 238 (2018).
- [17] A. Deltuva and R. Lazauskas, Phys. Rev. Lett. **123**, 069201 (2019).
- [18] A. Deltuva and R. Lazauskas, Phys. Rev. C **100**, 044002 (2019).
- [19] M.D. Higgins et al, Phys. Rev. Lett. **125**, 052501 (2020).
- [20] M.D. Higgins et al, Phys.Rev.C 103 (2021) 2, 024004, Phys.Rev.C 103 (2021) 2, 024004
- [21] S. Ishikawa, Phys. Rev. C **102**, 034002 (2020).
- [22] K. Fossez et al, Phys. Rev. Lett. **119**, 032501 (2017).
- [23] D.S. Petrov et al, Phys. Rev. Lett. **93**, 090404 (2004).
- [24] S.T. Rittenhouse et al, J. Phys. B: At. Mol. Opt. Phys. **44**, 172001 (2011).
- [25] S. Elhatisari et al, Phys. Lett. B **768**, 337 (2017).
- [26] A.M. Shirokov et al, Phys. Rev. Lett. **117**, 182502 (2016).
- [27] S. Gandolfi et al, Phys. Rev. Lett. **118**, 232501 (2017).
- [28] J.G. Li et al, Phys. Rev. C **100**, 054313 (2019).
- [29] L.V. Grigorenko, N. K. Timofeyuk and M. V. Zhukov, Eur. Phys. J. A **19**, 187 (2004).
- [30] R. Lazauskas and J. Carbonell, Front. in Phys. **7**, 251 (2020).
- [31] R. B. Wiringa, V. G. J. Stoks and R. Schiavilla, Phys. Rev. C **51**, 38 (1995)
- [32] E. Hiyama, R. Lazauskas, F. M. Marqués, J. Carbonell, Phys. Rev. C100, 011603 R (2019)
- [33] S.C. Pieper et al, Phys. Rev. C **64**, 014001 (2001)
- [34] R. Lazauskas, arXiv:1904.04675
- [35] S.A. Sofianos, S.A. Rakityansky and G.P. Vermaak, J. Phys. G 23, 1619 (1997).
- [36] We believe that the explanation of the recent experimental [4] data by supposing the existence of a 4n bound state is not sufficiently sound
- [37] The existence of singularities in the scattering amplitude is an implicit consequence of the scattering process itself. It follows from the Cauchy theorem that any analytic function in the full complex plane that vanishes at infinity, as it the case, should vanish everywhere and no scattering should exist.
- [38] See supplementary material provided to this work.

Supplementary material

In the four-body Faddeev-Yakubovsky (FY) formalism, the total wave function is decomposed in terms of the so called FY components. There are two type of components: the \mathcal{K} -type ones are built to properly implement the asymptotes of the 3+1 particle scattering channels, while the \mathcal{H} -type ones represent the 2+2 asymptotic channels (see figure 4). By permuting the particle indexes, one may construct 12-different components of \mathcal{K} -type and six different components of \mathcal{H} -type, i.e:

$$\Psi(\vec{x}, \vec{y}, \vec{z}) = \sum_{(i<j,k,l)=1}^4 \mathcal{K}_{ij,k}^l(\vec{x}, \vec{y}, \vec{z}) + \sum_{(i<j,k<l)=1}^4 \mathcal{H}_{ij}^{kl}(\vec{x}, \vec{y}, \vec{z}). \quad (15)$$

For a system of four identical particles (neutrons in the case we have considered) the different components of \mathcal{K} -type (idem for type- \mathcal{H}) become formally identical, satisfying the constrains imposed by the symmetry of identical particle permutation.

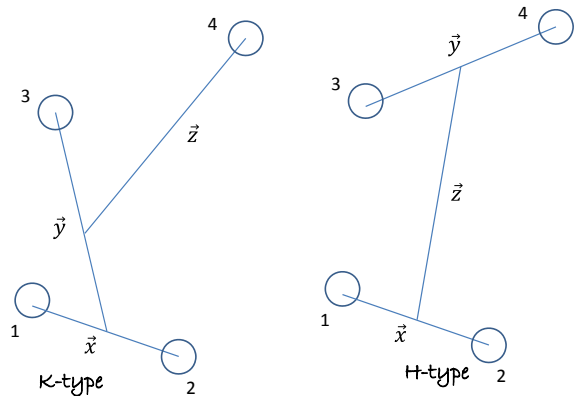


FIG. 4: 4-particle components $\mathcal{K}_{12,3}^4$ and \mathcal{H}_{12}^{34} together with the associated Jacobi coordinate sets.

It is difficult to analyze the fully antisymmetrized wave function of four-neutrons $\Psi(\vec{x}, \vec{y}, \vec{z})$, since the permutation operators blend together different geometrical configurations of the particles. Separate the non-symmetrical FY components offers much better insight. Our four-neutron calculations reveal a strong dominance of the \mathcal{H} -type components over the \mathcal{K} ones (by a factor close to 15 in ${}^8\text{He}$ wave function). This indicates the presence of strong 2n+2n correlations in the four neutron wave function, providing a doorway for the 2n+2n decay path. In figure 5, we depict the neutron densities of \mathcal{H} -component as a function of the distance between the two neutrons (r_{nn}) and the distance between the centers of mass of two dineutron pairs (r_{nn-nn}). The average distance (r_{nn-nn}) is significantly larger than (r_{nn}), indicating the formation of 2n+2n clustering. Furthermore, we may see that by increasing the core-neutron interaction

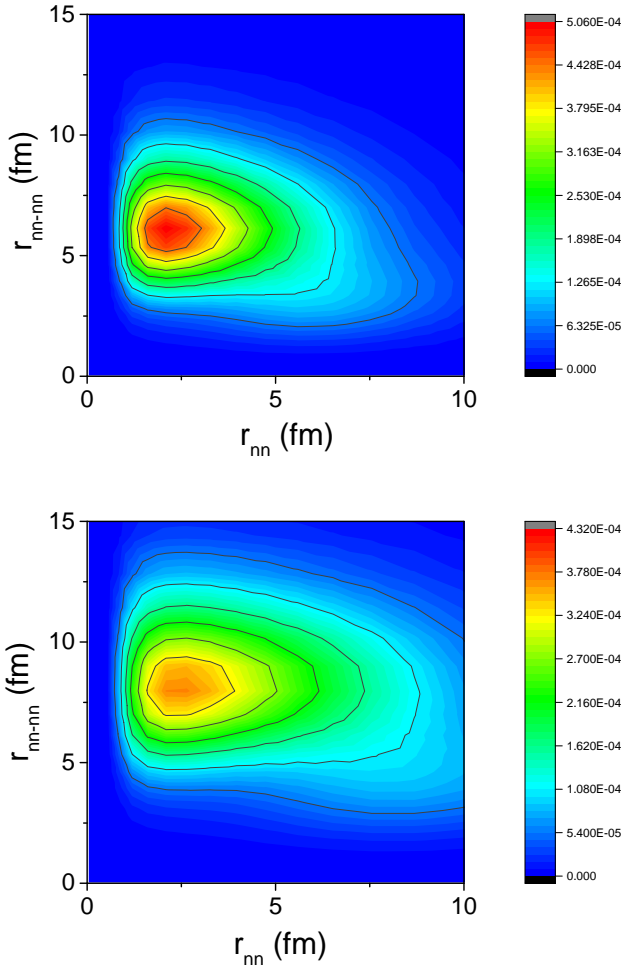


FIG. 5: Calculated halo neutron density distributions of the dominant 2+2 components in the ${}^8\text{He}$ wave function. These distributions are represented as a level surface plot of the two neutrons distance (r_{nn}) versus the distance between the centers of mass of two dineutron pairs (r_{nn-nn}). The results obtained with the AV18 nn interaction and with two different core-neutron interaction models are compared: the upper panel denotes the model with $\rho_0=2$ fm, while the lower panel corresponds to $\rho_0=3$ fm.

range (ρ_0), the average distance between two-dineutron clusters increases, whereas it almost does not affect the central value of r_{nn} . Note that the models using larger range parameter ρ_0 , bring the four-neutron missing mass distribution towards lower energies and makes it more compact. This last feature emphasizes the key role played by the 2n+2n configuration existing in the initial nucleus in order to get a sharp low energy structures in the four-neutron missing mass distribution.